CONF-790413--2

LA-UR-78-3050

TITLE: PREDICTION OF HIGH-ENERGY (> 0.3 MeV) SUBSTORM-RELATED MAGNETOSPHERIC PARTICLES

AUTHOR(S): D. N. Baker, R. D. Belian, P. R. Higbie, and E. W. Hones, Jr.

SUBMITTED TO: Proceedings of the International Solar-Terrestrial Predictions Workshop held in Boulder, CO April 23-27, 1979

los alamos scientific laboratory
of the University of California
LOS ALAMOS, NEW MEXICO 87545

DEPARTMENT OF ENERGY
CONTRACT W-7405-ENG. 36

PREDICTION OF HIGH-ENERGY (> 0.3 MeV) SUBSTORM-RELATED MAGNETOSPHERIC PARTICLES

D. N. Baker, R. D. Belian, P. R. Higbie and E. W. Hones, Jr
University of California, Los Alamos Scientific Laboratory
Los Alamos, New Mexico 87545

Measurements both at 6.6 R_E and in the plasma sheet ($\geq$ 18 R_E) show that high-energy substorm-accelerated particles occur preferentially when the solar wind speed (V_{sw}) is high. Virtually no > 0.3 MeV protons, for example, are observed in association with substorms that occur when V_{sw} is < 400 km/sec. On the other hand, the probability of observing high-energy protons is very large, both at geostationary orbit and in the plasma sheet, when V_{sw} is > 700 km/sec. These results suggest that realtime monitoring of interplanetary conditions could allow simple, effective prediction of high-energy magnetospheric particle disturbances.

INTRODUCTION

Measurable intensities of high-energy (0.3-2.0 MeV) substorm-related particles appear to be produced in only a small fraction (10-20%) of all substorms [Hones et al., 1976; Belian et al., 1978; Baker et al., 1978]. This occurrence frequency is generally found both for electrons [e.g. Paulikas and Blake, 1978] and for protons. Furthermore, particles of these energies occur with similar frequency both at synchronous altitude (6.6 R_E) in the outer radiation zone and in the distant plasma sheet ($\geq$ 18 R_E).

Absolute intensities of the high-energy particle component are generally rather low when compared to the fluxes of other substorm-accelerated particles. Nonetheless, the very energetic particles can be quite disruptive, when present, due to their penetrating character. Recent work has shown rather clearly the conditions under which such particles are produced, and in this paper we discuss simple methods for prediction of high-energy substorm particles from a knowledge of interplanetary plasma and magnetic field conditions.

INSTRUMENTATION

The measurements to be discussed in this paper were made with Los Alamos Scientific Laboratory instruments aboard several different earth-orbiting spacecraft. The Charged-particle Analyzer (CPA) instruments are on board spacecraft 1976-059A and 1977-007A which are both at the geostationary orbit. Energetic proton measurements made by various Vela spacecraft ($\sim$ 18 R_E) have been described previously by Hones et al. [1976].

The CPA instrument measures low-energy electrons (LoE) and low-energy protons (LoP). The respective energy ranges for the LoE and LoP subsystems are $30 \leq E_e \leq 300$ keV and $0.15 < E_p < 0.6$ MeV. The CPA also measures high-energy electrons (HiE) and high-energy protons (HiP). The HiE and HiP energy ranges are, respectively, $0.2 \leq E_e \leq 2.0$ MeV and $0.4 \leq E_p \leq 150$ MeV. Because the geostationary spacecraft under discussion here have no onboard magnetometers, pitch angle distributions of > 30 keV electrons are calculated in a self-consistent manner (see Higbie and Moomey [1977] and Higbie et al., [1978]). Using a spherical harmonic analysis and least-squares fitting technique, the symmetry axis of the second-order (pancake" or "cigar") pitch angle distribution of the > 30 keV electrons defines the local magnetic field direction. The colatitude (or meridional tilt) of the local field line calculated in this way is called θ_B; the second-order electron anisotropy amplitude is called C_2. ($C_2 < 0$ corresponds to a pancake distribution, whereas $C_2 > 0$ corresponds to a cigar distribution.)

BASIS OF THE METHOD

Figure 1 shows an example of one kind of high-energy proton enhancement commonly observed at the geostationary orbit. Early on October 2, 1976 several substorm "injections" of lower energy (< 300 keV) protons and electrons were detected by CPA instrumentation aboard spacecraft 1976-059. Notable among these injections was that which occurred at ~ 0420 UT when spacecraft 76-059 was at ~ 0200 LT. As seen in Figure 1, this injection event had associated with it protons extending in energy up to at least ~ 1.0 MeV.

At the higher energies (generally > 300 keV) the injected protons appeared in the form of rather narrow, well-defined pulses of particles. Significant dispersion is seen since higher energy channels show flux increases before similar increases are seen at lower energies. Note that in each energy range there are several clear pulses, or "echoes," as the protons drift azimuthally around the earth [Belian et al. 1978].

As seen by the parameter θ_B the local magnetic field was in a very stretched, or taillike, configuration prior to ~ 0430 UT, but this relaxed toward a somewhat more dipolar configuration after the particle injection.

The highly disturbed geomagnetic conditions observed during the early portion of October 2 are seen in the Meanook and Great Whale River magnetogram traces shown in Figure 2. Especially noteworthy is the very large negative bay in the Great Whale H-component beginning at ~ 0420 UT. This substorm enhancement is plausibly related to the proton injection observed at 6.6 R_E.

We find both drift-echo (DE) and nondrift echo (NDE) types of proton enhancements at geostationary orbit. In contrast to the DE type of event shown after ~ 0420 UT in Figure 1, NDE events show clear flux enhancements but by definition there is not a very evident pulsed behavior of high-energy protons in these cases.

In Figure 3 we show several different kinds of data. The upper two panels of the figure show daily averages, respectively, of the proton and electron intensities measured by the CPA aboard spacecraft 76-059. Selected energy

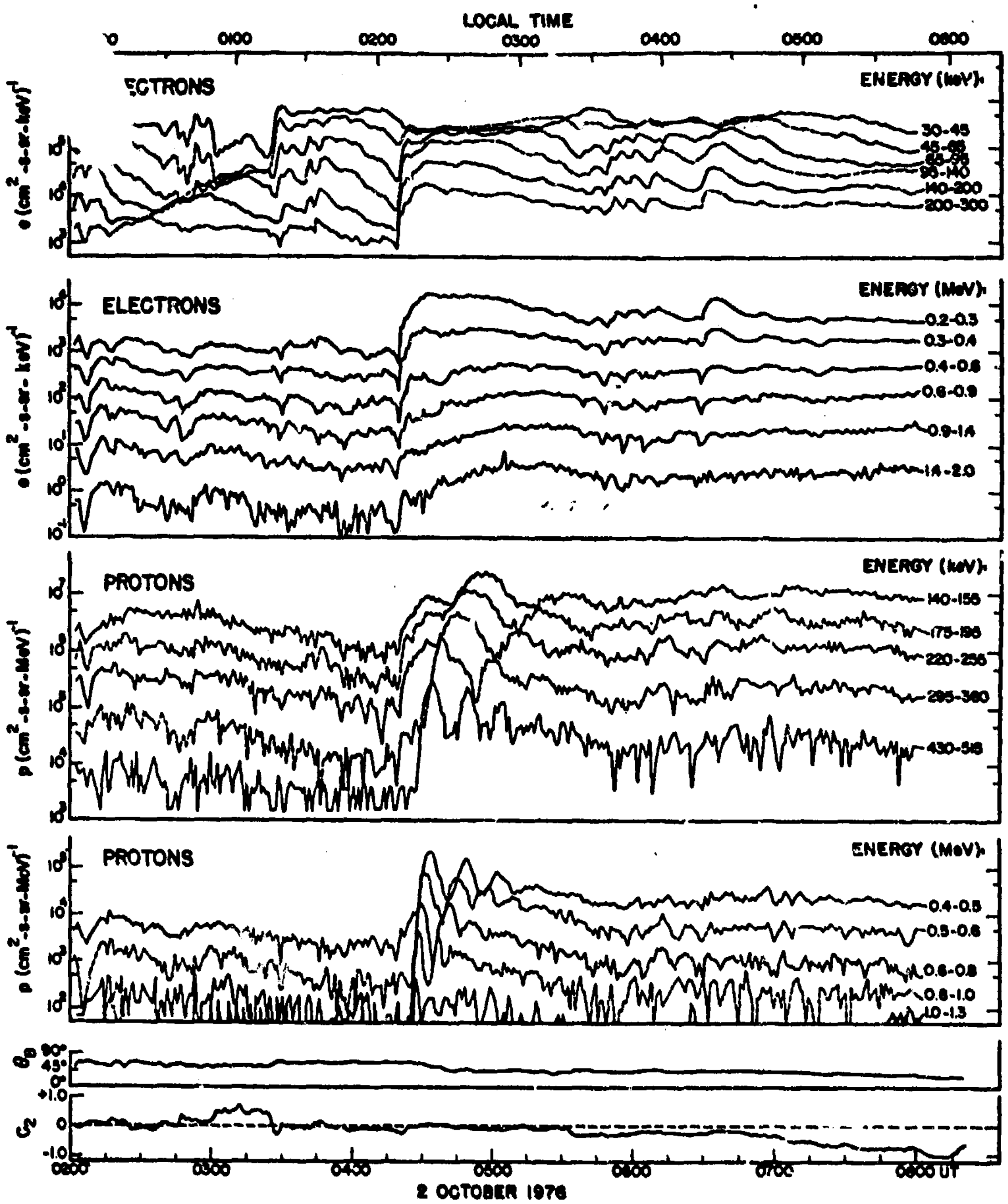

Figure 1. Selected CPA data from spacecraft 1976-059A for a portion of October 2, 1976 including electrons in various energy ranges (as labeled) in the upper two panels and protons in the third and fourth panels from the top. The bottom two panels contain information (as described in the text) obtained from the low-energy electron anisotropies: θ_B is the inferred local magnetic field direction and C_2 is the > 30 keV electron second-order anisotropy amplitude. A major feature seen in these data is high-energy proton drift-echo event beginning at ~ 0420 UT (and at a spacecraft local time of ~ 0200).

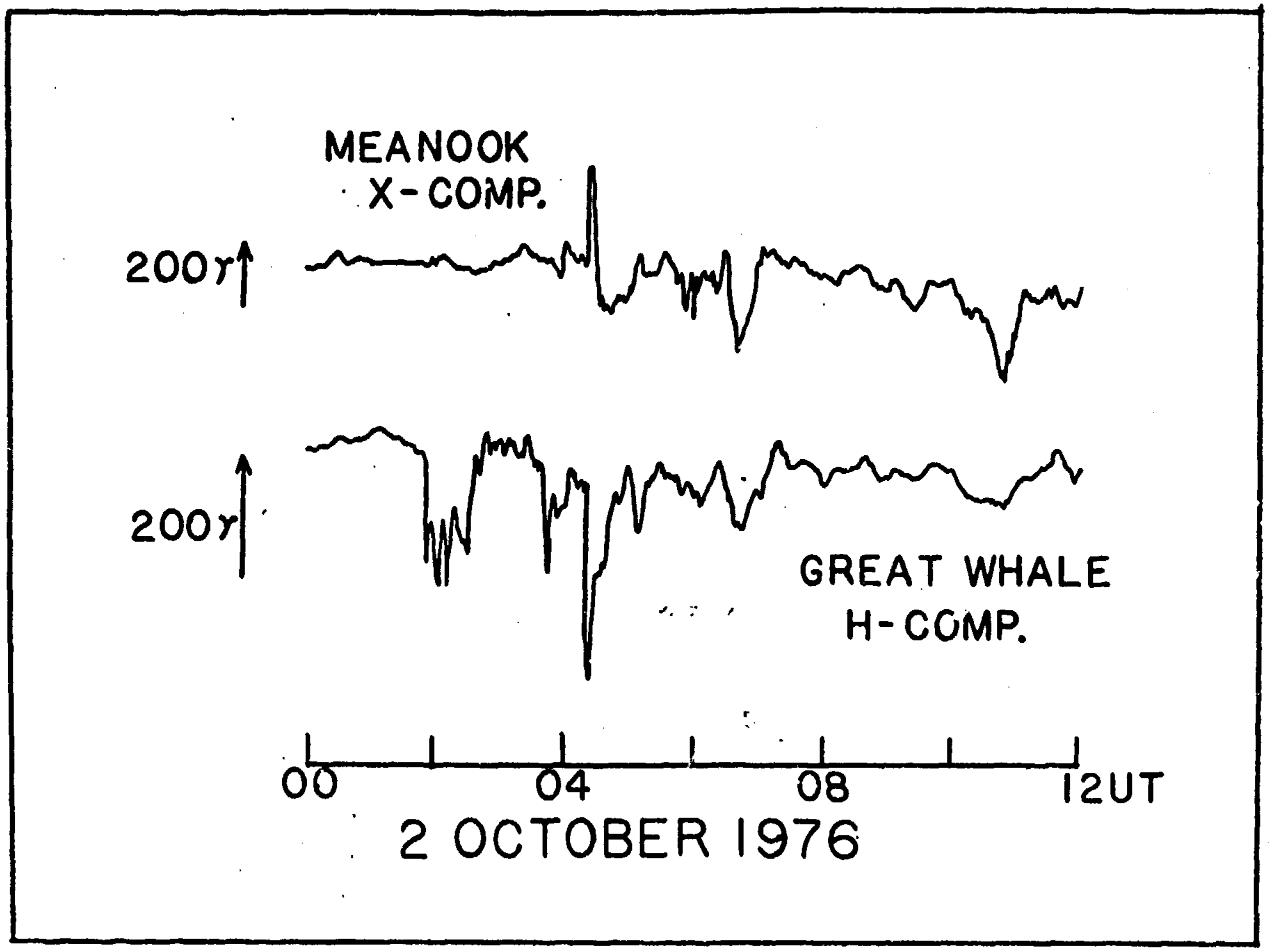

Figure 2. Ground-based magnetogram traces from Meanook (reaches magnetic midnight at 0900 UT) and Great Whale River (midnight at 0600 UT) showing substorm activity early on October 2, 2976.

ranges (out of many available) are shown for a two month period, viz., November-December 1976. Also shown are the 12-hour averages of the solar wind speed, V_{sw} (third panel), the interplanetary ~ 1 MeV proton flux (fourth panel), the daily number of DE plus NDE events seen at spacecraft 76-059 (fifth panel), and finally, the K_p daily sum (sixth panel).

As may be seen, K_p generally correlates with V_{sw}. More importantly here, however, it is also suggested by Figure 3 that synchronous altitude high-energy proton and electron flux profiles, the number of DE and NDE proton events, and even interplanetary energetic proton bursts correlate fairly well with V_{sw}.

The correlation of high-energy proton enhancements at 6.6 R_E with solar wind speed is summarized in a statistical fashion in Figure 4. The upper panel of the figure shows the solar wind speed occurrence distribution for a one-year period (July 1976-June 1977). The raw numbers of DE and NDE events seen during various solar wind speed intervals are shown in the second panel. Finally, by normalizing the panel 2 distributions by the distribution in panel

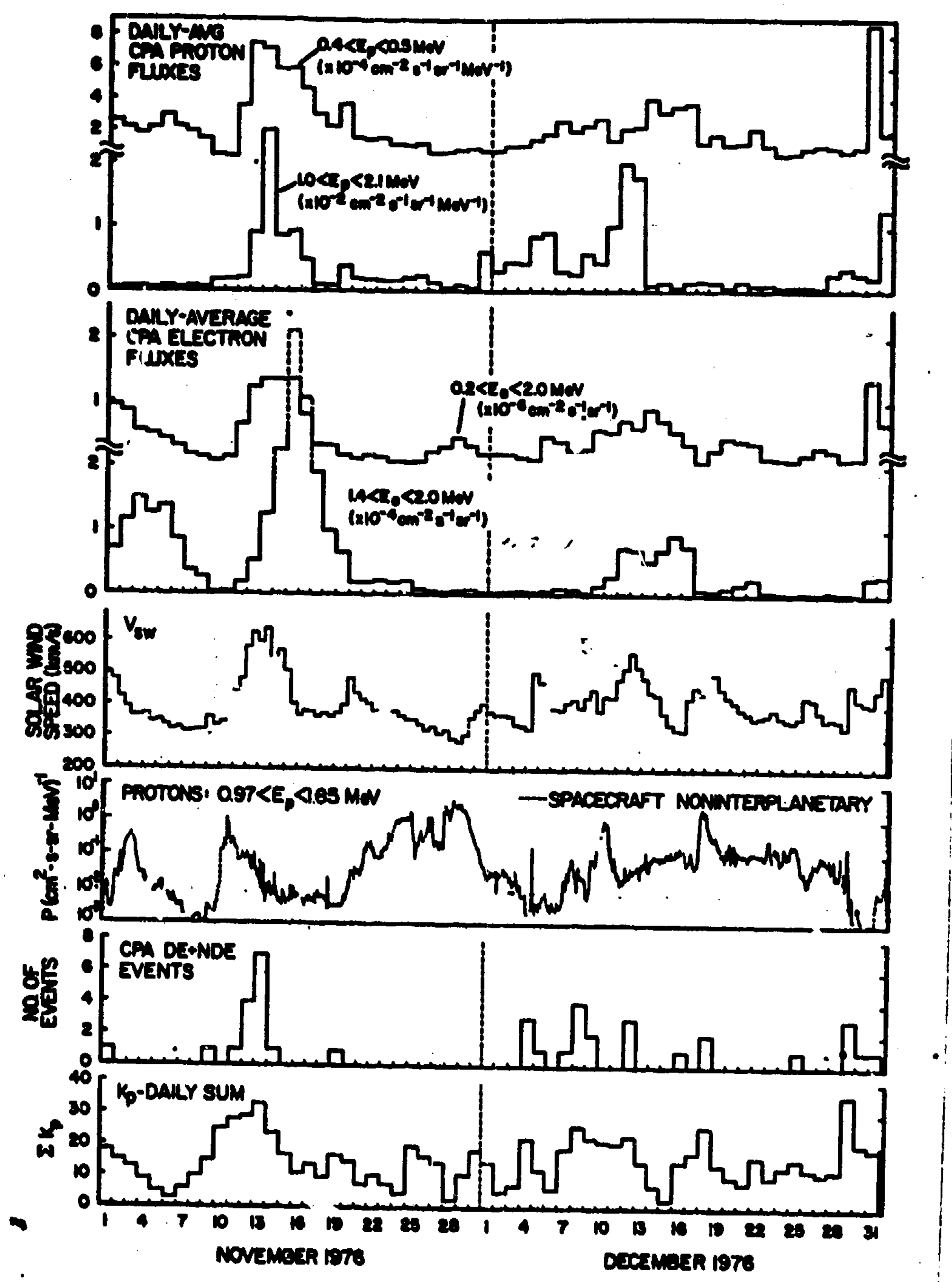

Figure 3. A composite plot of various data sets for November and December of 1976. The upper two panels show, respectively, CPA proton and electron flux profiles at 6.6 R_E. The third panel shows the 12-hour solar wind speed averages (courtesy of J. R. Asbridge, S. J. Bame, W. C. Feldman, and J. T. Gosling). The fourth panel shows the interplanetary flux of 0.97-1.85 MeV protons (Solar-Geophysical Data). The fifth panel shows the daily number of CPA high-energy proton events observed during the period. Finally, the bottom panel shows the November-December K_p daily sum, ΣK_p. As discussed in the text, several correlations between the various data sets are evident.

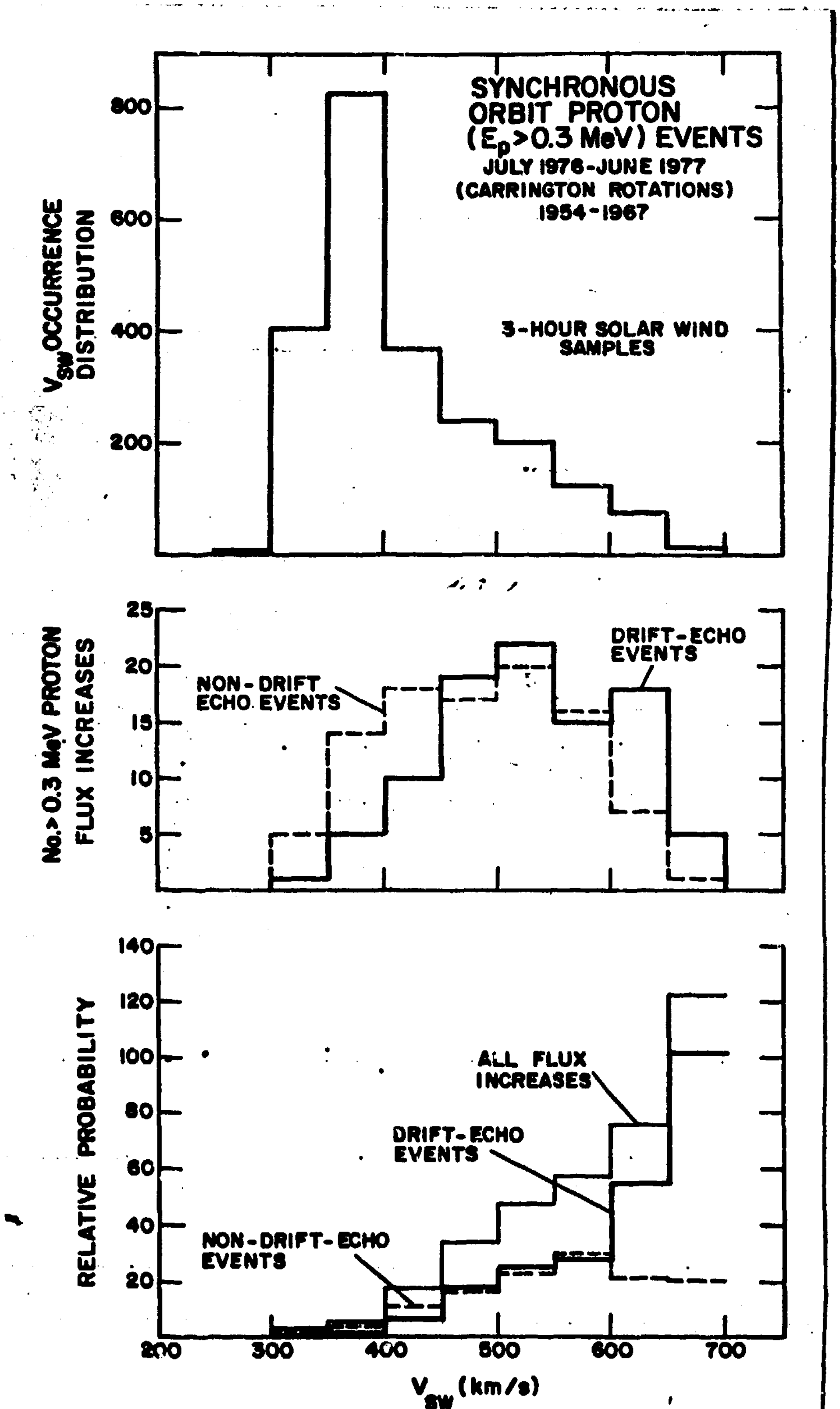

Figure 4. The upper panel shows that between July 1976 and June 1977 the bulk solar wind speed occurrence distribution peaked strongly between 350 and 400 km/sec. The second panel shows that most DE and NDE events occurred when V_{sw} was > 400 km/sec. When panel 2 data are normalized by the data of panel 1, a strong positive correlation is found between proton flux increases at 6.6 R_E and solar wind speed as shown in panel 3.

1, we get the relative occurrence probability of high-energy proton events at synchronous orbit.

We see that although V_{sw} is < 400 km/sec much of the time during 1976-77, relatively speaking almost no high-energy proton enhancements occur during these low-speed conditions. However, as V_{sw} increases above 400 km/sec the probability of observing a high-energy proton enhancement increases dramatically.

This dependence on solar wind speed is not restricted to 6.6 R_E. As seen in Figure 5, very similar results obtain for high-energy proton events observed in the plasma sheet by Vela instrumentation. In the third panel of Figure 5 we have normalized the probability to 100 for the 650-700 km/sec interval. Notice the change in scale and the very strong increase in relative probability when V_{sw} > 700 km/sec.

Not only the number of substorm-related events depends on solar wind speed, but also the absolute intensity of each event depends on the associated V_{sw}. This is demonstrated in Figure 6 which shows the observed peak proton intensities measured by the CPA plotted versus V_{sw}. We have broken the observations into three sectors according to the spacecraft location at the time the drift-echo events were detected. As discussed by Baker et al. [1978], the local time variation seen in Figure 6 may be related to dispersion effects as particles move away from injection regions and also may reflect drift-shell effects due to strong cross-magnetospheric electric fields. Nonetheless, a substantial positive correlation between peak flux and solar wind speed is seen in each local time sector.

Finally, we also find magnetospheric high-energy proton enhancements to have a noticeable tendency to occur when the interplanetary magnetic field (IMF) is southward. As shown by the statistical results related to Vela observations in Figure 7, the total IMF magnitude is not abnormally large during these events (panel (a)). However, panel (b) shows that ~ 95% of the Vela events occurred following at least a one-hour period of predominantly southward IMF (B_z < 0). Panels (c) and (d) show the occurrence frequency and median observed 0.5 MeV fluxes, respectively, plotted versus the combination of the observed V_{sw} and B_z for each event (i.e., the Y-component of the interplanetary electric field, IEF). Substantial dependences on the magnitude of the dawn-to-dusk component of the interplanetary electric field (IEF) are suggested.

DISCUSSION AND POSSIBLE USES

The foregoing results suggest rather strongly that realtime monitoring of the interplanetary plasma and magnetic field could permit a quite simple and useful prediction scheme. As a minimum, users who wished to know whether or not substorm-related particles of hundreds of keV (or above) could be expected need only find out the solar wind velocity. This seems to be the simplest and most fundamental correlation: if V_{sw} is low, say < 400 km/sec, then high-energy, substorm-accelerated particles are extremely unlikely throughout the outer magnetosphere; conversely, if V_{sw} is very high, say $\geq$ 700 km/sec, then

5

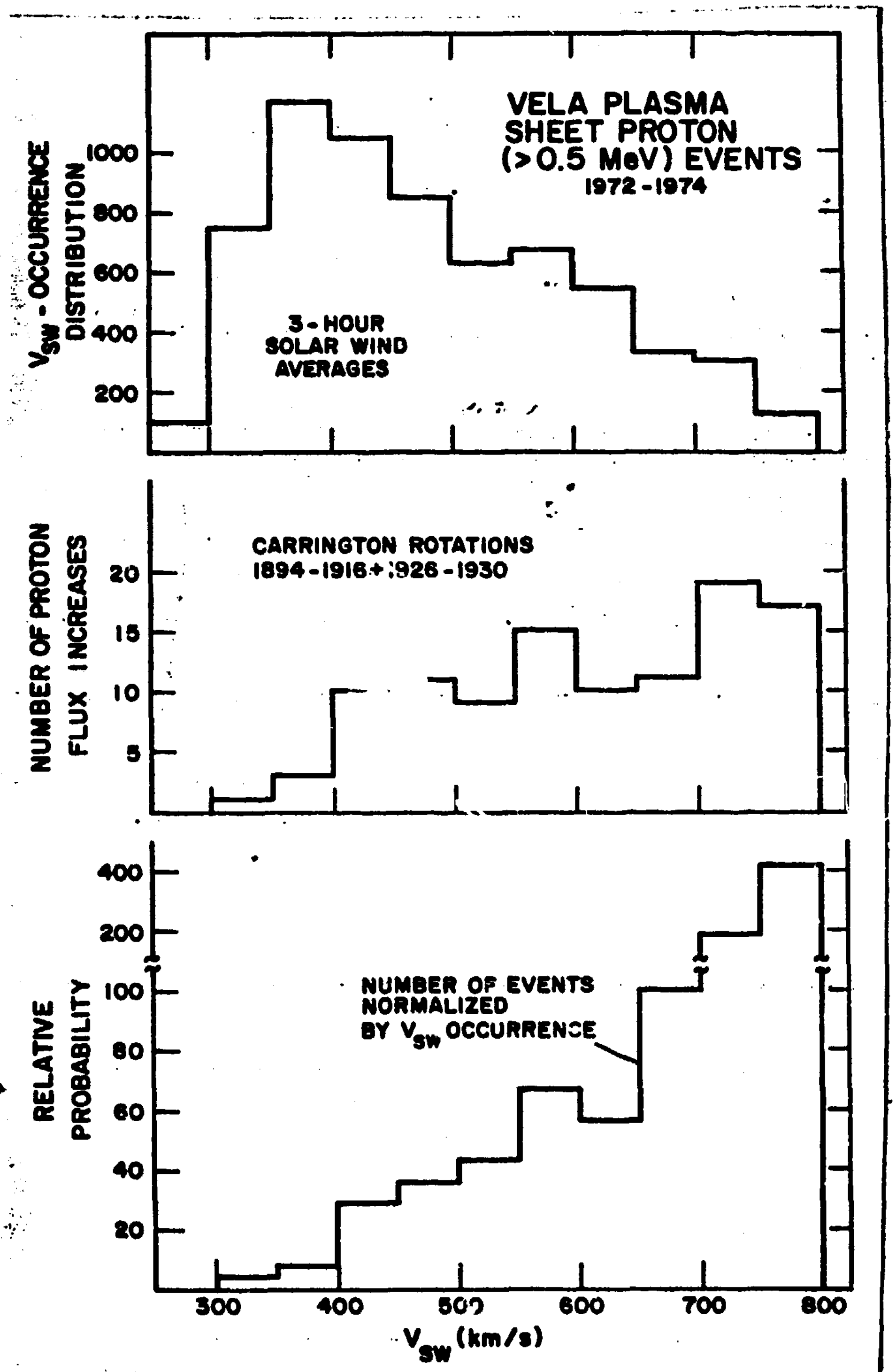

Figure 5. Data similar to Figure 4, but for Vela plasma sheet proton enhancements. In the lower panel we have normalized the relative probability to 100 between 650 and 700 km/sec. The relative probability of a high-energy proton event increases dramatically at high V_{sw}.

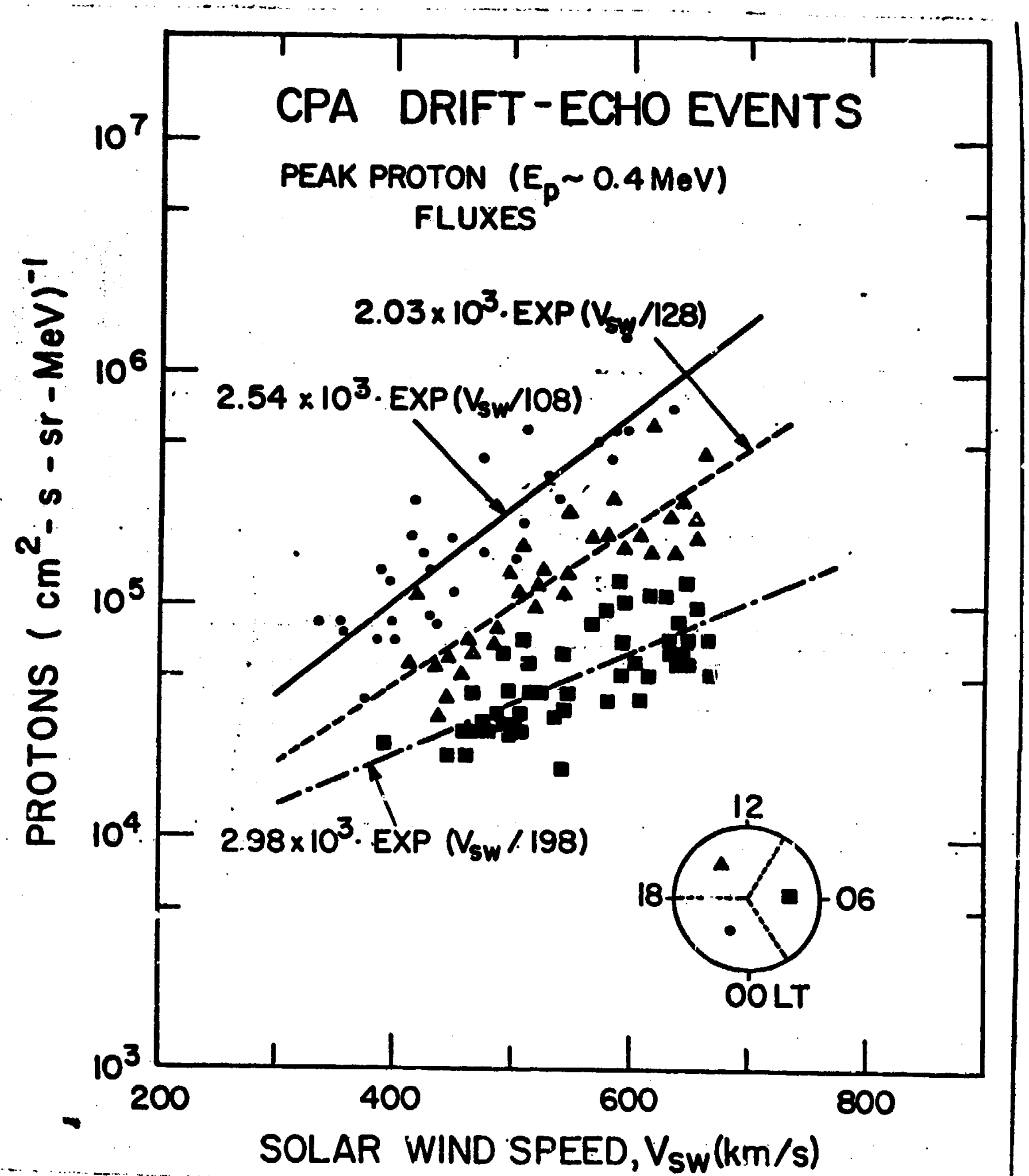

Figure 6. Peak observed CPA proton fluxes (at $E_p \sim 0.4$ MeV) versus bulk solar wind speed. A positive correlation is shown by the linear regression fits to data from each local time sector.

the probability is very high that a substorm will produce copious quantities of high-energy protons and electrons.

There may be deeper and more detailed correlations that can be inferred (cf., Figure 7). These more quantitative correlations appear to require knowledge of the IMF, as well as V_{sw}. Furthermore, there may be some specific feature, such as the fluctuation spectrum of the IMF, the IEF, etc., which

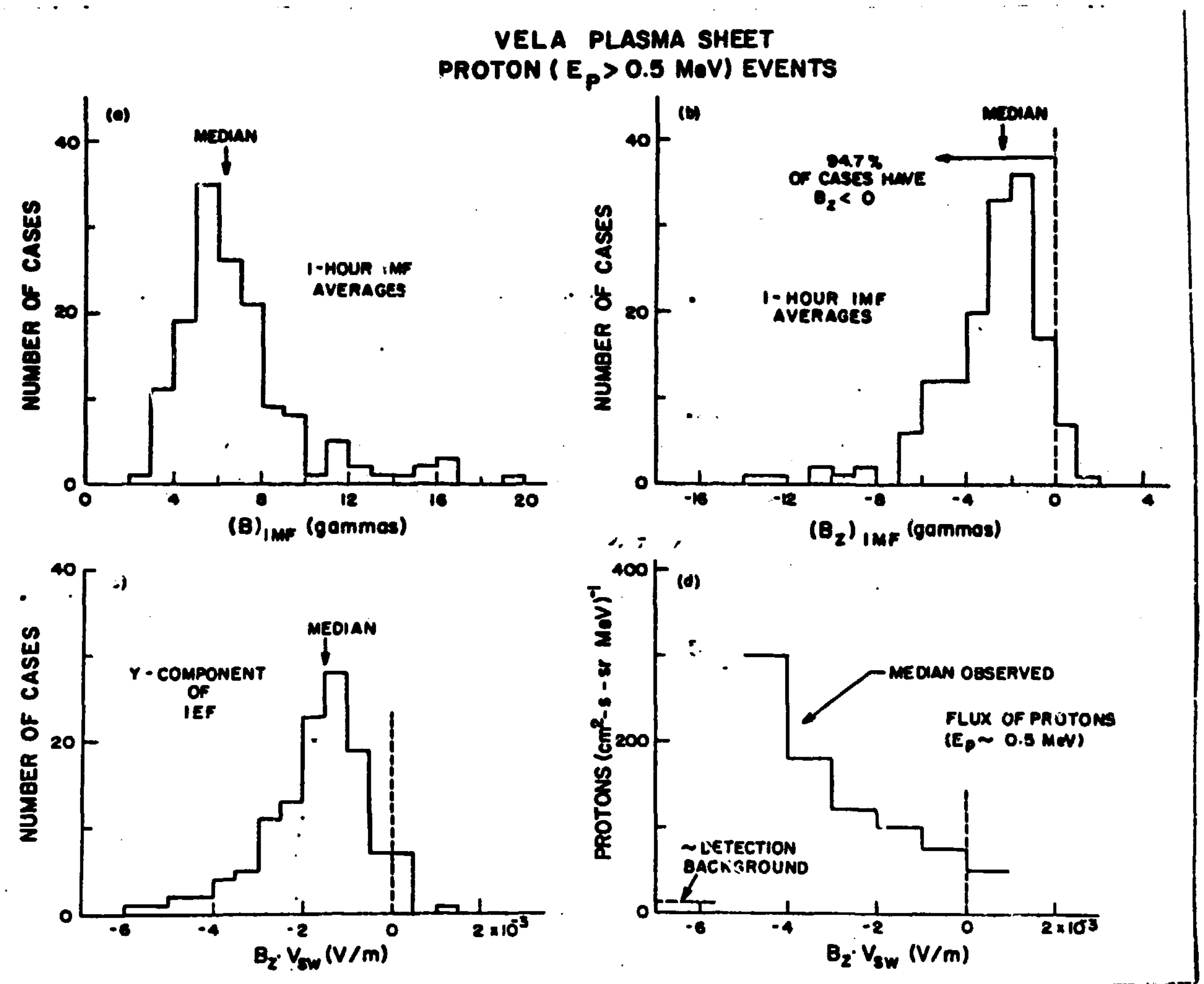

Figure 7. The dependence of Vela plasma sheet proton event occurrence fre- quencies: (a) on the total interplanetary mangetic field (IMF) streng , on the north-south IMF component, $(B_z)_{IMF}$; and (c) on the Y-component the interplanetary electric field (IEF) which is the negative of $(B_z)_{IMF}$ V_{sw}. Part (d) shows the median observed peak proton flux in the plasma sheet versus $B_z V_{sw}$.

actually "produces" the large acceleration events observed when V_{sw} is high. Nonetheless, our results suggest that whatever the mechanism, it occurs only when solar wind speed is high; other IP changes appear to contribute in a secondary way to this feature.

In summary, it appears that a real time monitoring of V_{sw} and the IMF could provide both a qualitative and a quantitative prediction of the proba- bility for the occurrence and intensity of > 0.3 MeV substorm related ener- getic particles. These predictions would seem to have validity both in the outer radiation zones (L ~ 5-8) and in the magnetotail.

ACKNOWLEDGMENTS

We particularly thank S. J. Bame, J. R. Asbridge, W. C. Feldman, and J. T. Gosling for providing us with solar wind data used in this study. This work was done under the auspices of the United States Department of Energy.

BIBLIOGRAPHY

Baker, D.N., R. D. Belian, P. R. Higbie, and E. W. Hones, Jr., High-energy magnetospheric protons and their dependence on geomagnetic and interplanetary conditions, submitted to J. Geophys. Res., 1978.

Belian, R. D., D. N. Baker, P. R. Higbie, and E. W. Hones, Jr., High-resolution energetic particle measurements at 6.6 R_E, 2, High-energy proton drift-echoes, J. Geophys. Res., 83, 1978.

Higbie, P. R. and W. R. Moomey, Pitch angle measurements from satellites using particle telescopes with multiple view directions, Nucl. Instr. and Meth., 146, 439, 1977.

Higbie, P. R., R. D. Belian, and D. N. Baker, High-resolution particle measurements at 6.6 R_E, 1, Electron micropulsations, J. Geophys. Res., 83, 1978.

Hones, E. W., Jr., I. D. Palmer, and P. R. Higbie, Energetic protons of magnetospheric origin in the plasma sheet associated with substorms, J. Geophys. Res., 81, 3866, 1976.

Paulikas, G. A., and J. B. Blake, Energetic electrons at synchronous altitude 1967-1977, Aerospace Corporation Rep. No. TR-0078 (3960-05), March 1978.

Solar Geophysical Data, Environmental Data Service, NOAA, Nos. 393 and 394, May-June, 1977.